PNAS
www.pnas.org

Supplementary Information for

Spontaneous Formation of Multilayer Refractory Carbide Coatings in a Molten Salt Media

Loic Constantin,[1,2,] Lisha Fan,[1,] Mathilde Pouey,[2] Jérôme Roger,[3] Bai Cui,[4] Jean-François Silvain[1,2]* and Yong Feng Lu,[1]*

[1]Department of Electrical and Computer Engineering, University of Nebraska-Lincoln, Lincoln, Nebraska, 68588-0511, United States

[2]CNRS, Univ. Bordeaux, Bordeaux INP, ICMCB, UPMR 5026, F-33608 Pessac, France

[3]Université de Bordeaux, Laboratoire des Composites Thermo Structuraux – LCTS 3 allée de la Boétie, F-33600 Pessac Cedex, France

[4] Department of Mechanical and Materials Engineering, University of Nebraska-Lincoln, Lincoln, NE 68588-0526, USA.

1. Molten salt coating

Figure S1 illustrates the different steps involved in the molten salt process. First, the salt and the metal; titanium and or chromium were homogeneously mixed using an agate mortar. The carbon fibers (CFs) were then introduced into the salt/metal mixture and manually shaken. Subsequently, the mixture was deposited on an alumina crucible, as shown in Step 1. The crucible was placed in a tubular furnace under an argon flux at a temperature range between 800 and 950 ºC for different time periods, ranging from 0.5 to 5 h, as illustrated in Step 2. When the oven cooled down, the salt was dissolved in boiling water. The coated CFs were recovered by filtration, as illustrated in Steps 3 and 4. Finally, the coated CFs were dried in an oven at 60 ºC for 1 h.

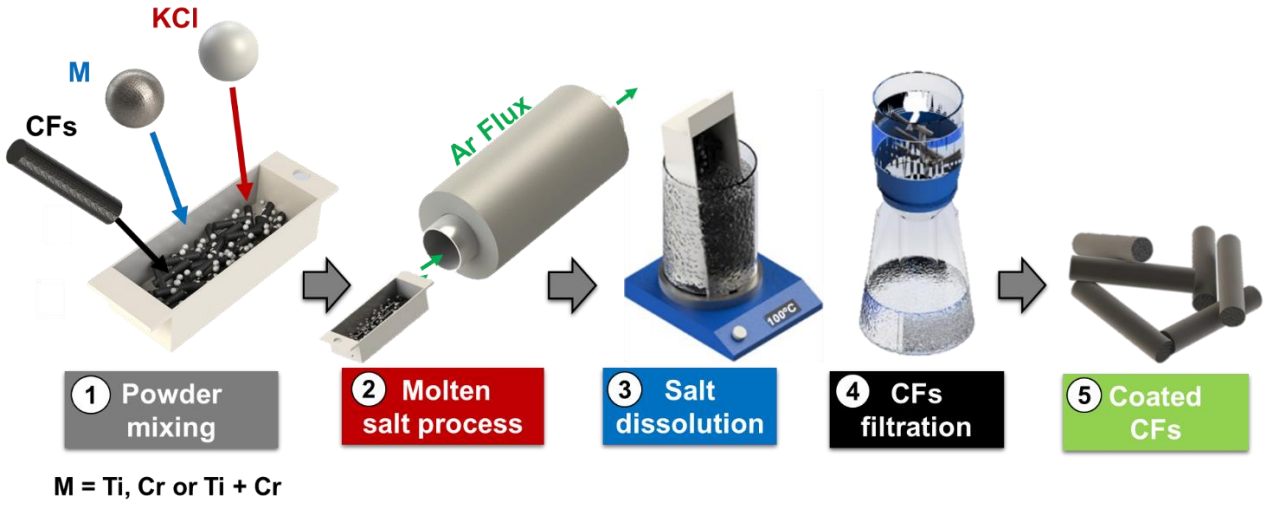

Figure. S1. Schematic illustration of the molten salt coating process: 1) mixing M (Ti, Cr, or Ti+Cr), KCl salt, and CFs; 2) oven synthesis at 950 ºC for 5 h; 3) salt dissolution in boiling water, 4) filtration and recovery of coated CFs, and 5) drying coated CFs in an oven at 60 ºC.

2. SEM micrographs of fibers surfaces

Figure S2 presents the fiber surfaces after being coated with M = titanium (Ti) (TiC), chromium (Cr) (Cr_3C_2), or Cr + Ti (Cr_3C_2-TiC-Cr_3C_2). As can be noted, the coated layers are homogenous on all fibers for each coating.

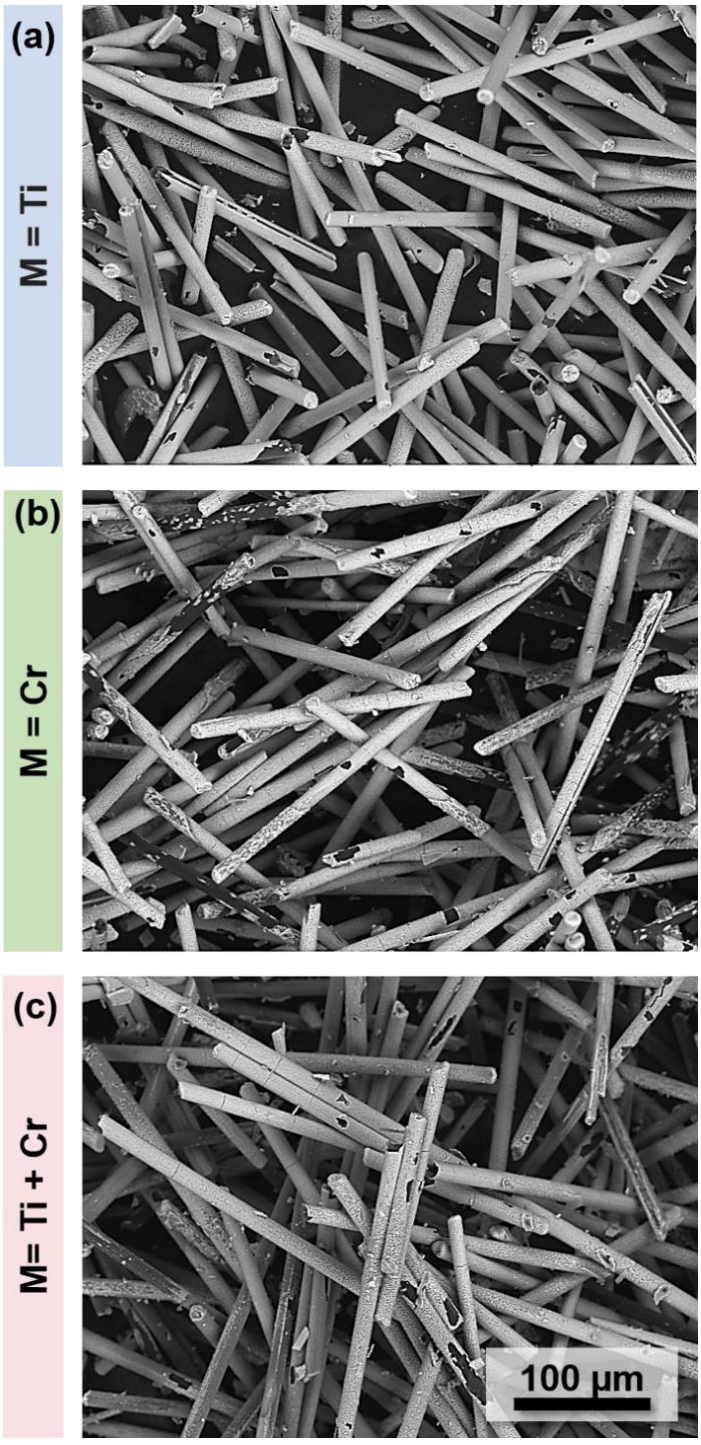

Figure. S2. SEM micrographs of the fibers' surface for **(a)** M= Ti (TiC), **(b)** M= Cr (Cr_3C_2), and **(c)** M = Ti+ Cr (TiC-Cr_3C_2-TiC).

3. XRD diffractogram after salt quenching

In addition to the SEM micrographs presented in **Fig. 3**, the products were studied by XRD, as presented in **Fig. S3**. It can be noticed that after a few seconds of coating, Cr_3C_2 and TiC peaks were observable with the presence of titanium oxide (TiO_x) and Cr (unreacted powders). After 10 min, peak intensities of TiC increased while Cr_3C_2 peaks decreased. The change in the intensity was presumably due to the creation of the TiC layer above the inner Cr_3C_2 layer. After 20 min, the TiC peaks reached their maximum. No TiO_x was observed, suggesting their complete reaction. However, peaks from Cr powders were still noticed. After 30 min, the peaks from Cr_3C_2 increased; and the TiC peaks decreased (due to the formation of Cr carbide above them). Also, Cr powders were noticed, suggesting their partial reaction.

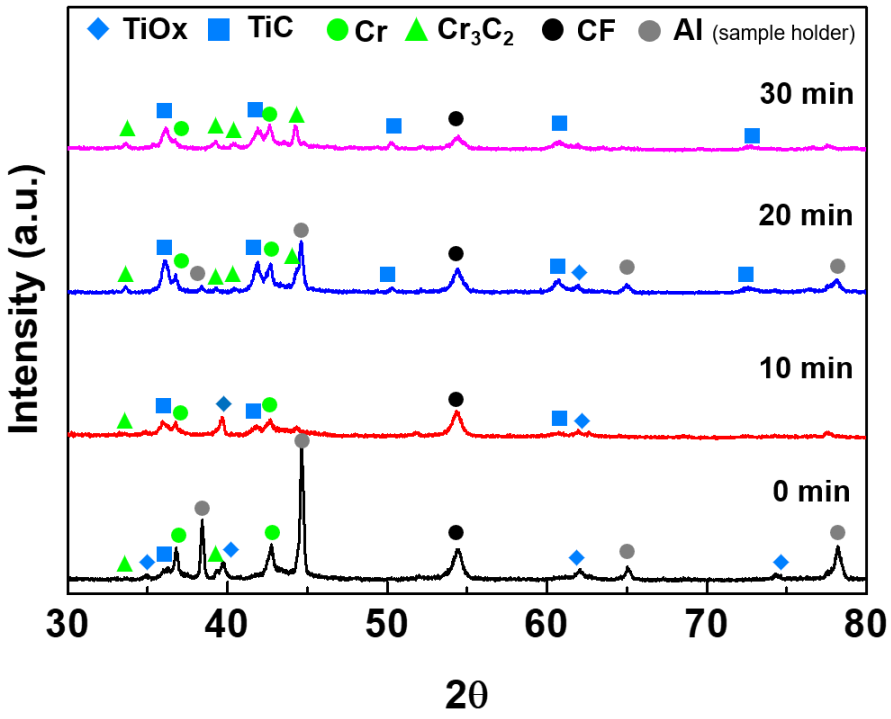

Figure. S3. XRD diffractogram of the quenched CFs after salt dissolution for different coating times between 0 and 30 min.

4. Kinetic growth of TiC and Cr_3C_2 systems

The kinetic growth of single carbides (M= Ti, Cr) was studied at different temperatures and times ranging from 800 to 950 ºC for 1 to 5 h, respectively. After coating under different conditions, the coating thicknesses on the CFs were measured from the cross-sectional views of the coated fibers (**Fig. S4 and S5)** and plotted in **Fig. S6.** As can be seen, a linear relationship between the thickness of the carbide layers and the square roots of the coating times was found. In classical kinetics, it can be described by the following equation (1, 2):

$$x = \sqrt{D_{eff}T}, \quad \textbf{(1)}$$

where x is the thickness of the carbide layer [cm], t is the time [s], and D_{eff} is the effective diffusion coefficient [cm^2/s]. The D_{eff} was retrieved from the slopes of the curves under all conditions. It was found that the D_{eff} varied from $3.8.10^{-13}$ to $1.3.10^{-11}$ m^2/s and $3.6.10^{-13}$ to $4.4.10^{-12}$ m^2/s in the temperature range of 800 to 950 ºC for TiC and Cr_3C_2, respectively. Likewise, Cr had an effective diffusion coefficient similar to Ti at 800 ºC and was three times larger at 950 ºC. These values confirm that the diffusion of Cr was faster than Ti in molten potassium chloride (KCl) at 950 ºC.

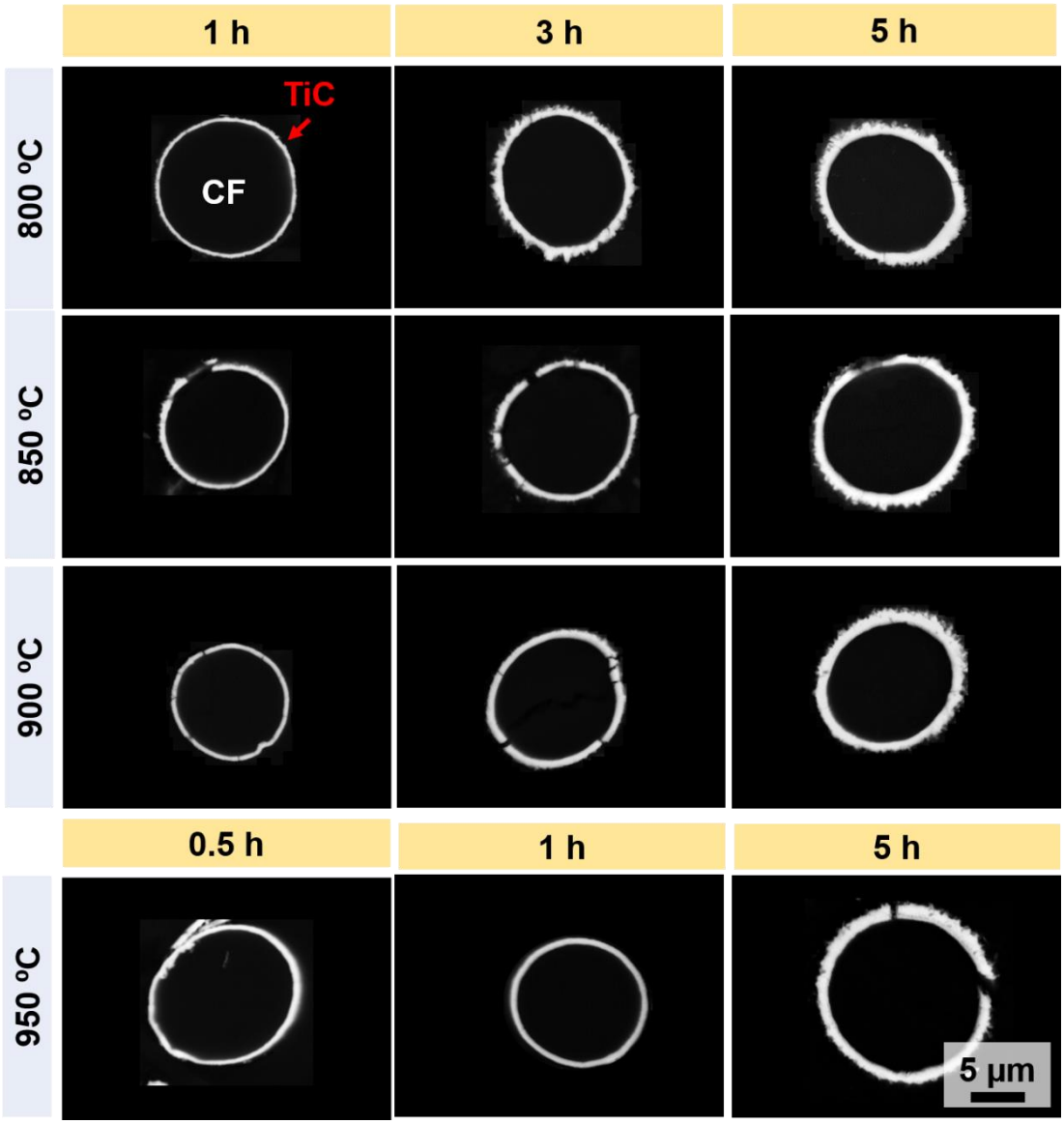

Figure. S4. BSE mode SEM cross-sectional views of CFs coated with TiC for 1 to 5 h at 800, 850, 900, and 950 ºC for different times between 0.5 and 5 h.

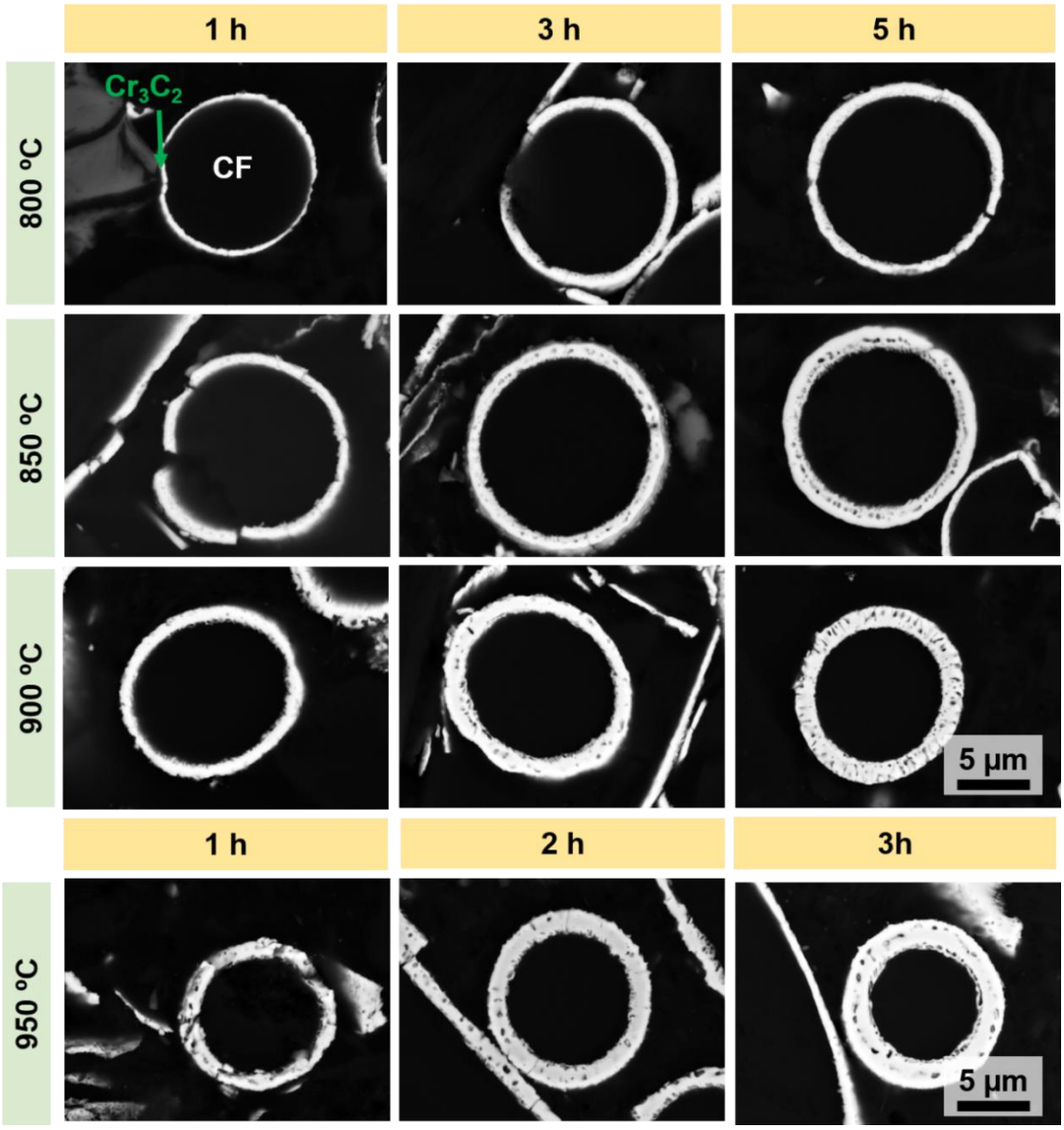

Figure. S5. BSE mode SEM cross-sectional views of CFs coated with Cr_3C_2 for 1 to 5 h at 800, 850, 900, and 950 ºC for different times between 1 and 3 h.

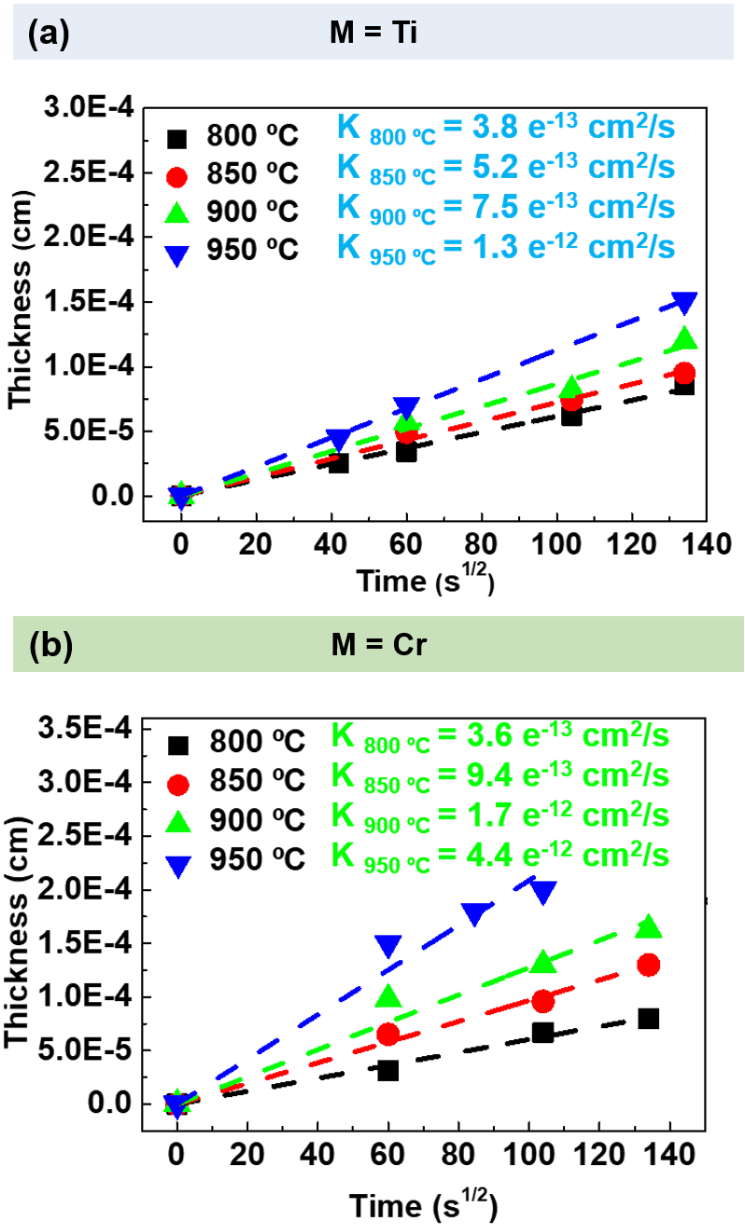

Figure. S6. Coating thickness vs. square root of time for **(a)** M = Ti (TiC) and **(b)** M = Cr (Cr_3C_2).

5. Oxidization tests of TiC, Cr_3C_2, and Cr_3C_2 – TiC – Cr_3C_2

Raman spectroscopy was performed to identify the oxidation reaction of carbide layers before and after being subjected to the oxyacetylene flame. **Figure S7a** presents Raman spectra before and after the oxidation test for M = Ti (TiC). Before the oxidation test, peaks around 262, 394, and 602 cm^{-1} were observed and attributed to TiC (3). After the oxidation test, the TiC peaks remained but with an additional peak at 146 cm^{-1} attributed to titanium dioxide (TiO_2) (4). **Figure S7b** shows the Raman analyses for M =

Cr (Cr_3C_2). No peaks were found on the coated layer due to the absence of the Raman signal for Cr carbides. Nevertheless, after the oxidation test, two peaks appeared around 548 and 856 cm^{-1} that were attributed to Cr_2O_3 and CrO_3, respectively (5). Finally, **Fig. S7c** shows the Raman spectra for a coating using M = Ti + Cr. Before the oxidation test, small peaks of TiC were observed, while after the oxidation test, a peak around 548 cm^{-1} appeared and was attributed to Cr_2O_3.

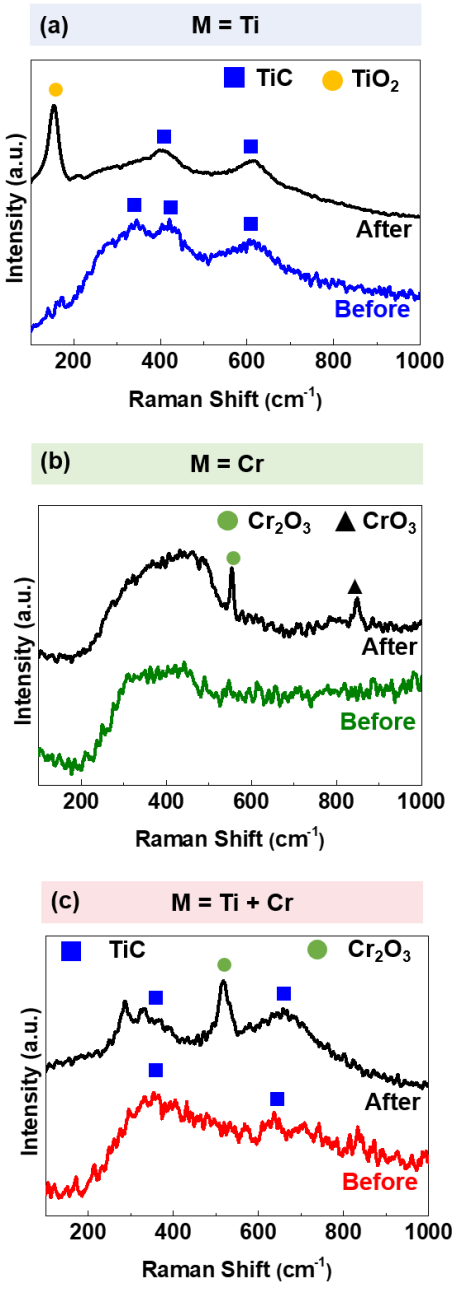

Figure S7. Raman spectra before and after the oxidation test for **(a)** M = Ti, **(b)** M = Cr and **(c)** M = Ti + Cr.

Figure S8, S9 and **S10** present SEM micrographs, EDS analysis of the coated CFs with M = Ti, Cr, and Ti + Cr after fire exposure. As can be observed, when M = Ti and Cr, about 70 % at. Impart for oxygen at the surface of the coating, implying the formation of oxide. However, when M = Ti + Cr, the quality of oxygen drops to 40 at.% and where it is preferentially located where Cr is detected (**Figure S10 (c)**).

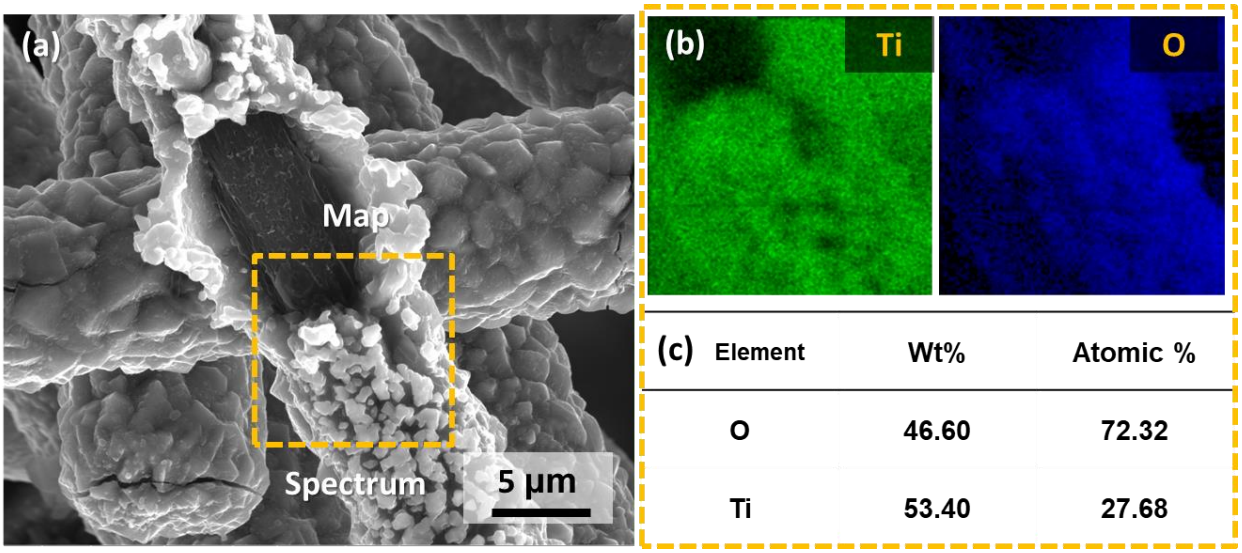

(c)

Element	Wt%	Atomic %
O	46.60	72.32
Ti	53.40	27.68

Figure S8. **(a)** SEM micrographs of coated CFs with M = Ti after fire exposure, **(b)** EDS maps of the coated CFs, and **(c)** EDS quantification of EDS map area

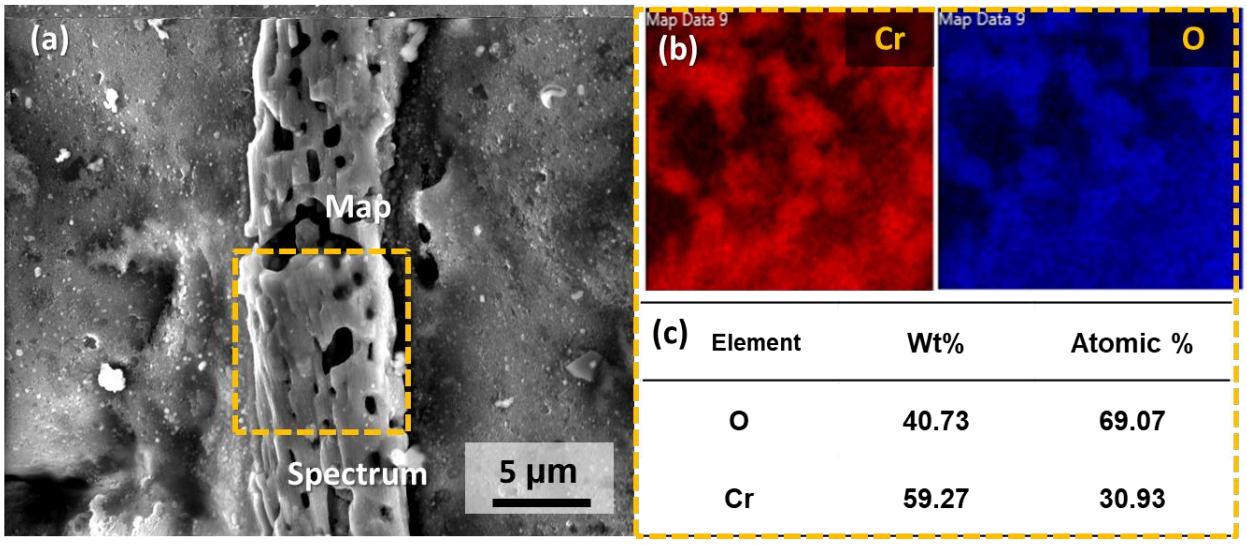

(c)

Element	Wt%	Atomic %
O	40.73	69.07
Cr	59.27	30.93

Figure S9. **(a)** SEM micrographs of coated CFs with M = Cr after fire exposure, **(b)** EDS maps of the coated CFs, and **(c)** EDS quantification of EDS map area

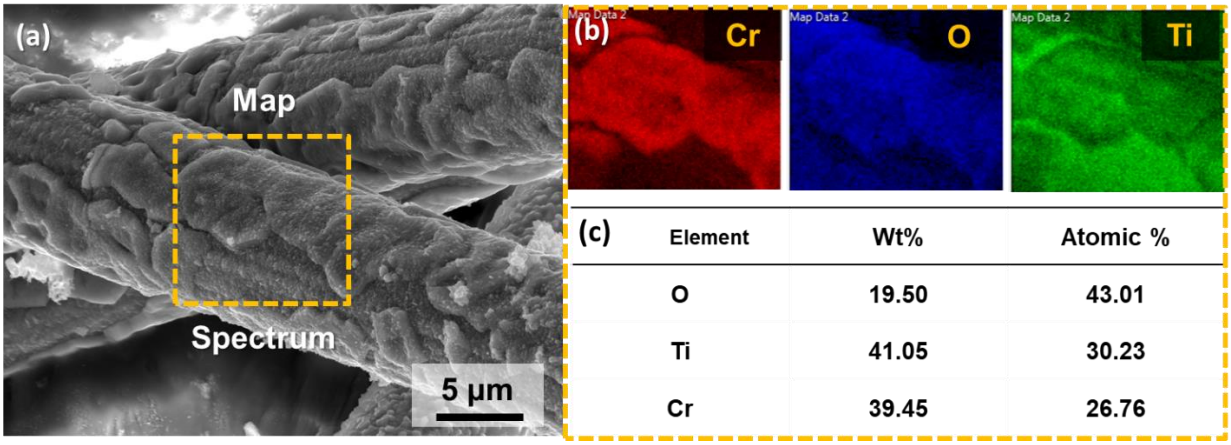

(c)

Element	Wt%	Atomic %
O	19.50	43.01
Ti	41.05	30.23
Cr	39.45	26.76

Figure S10. **(a)** SEM micrographs of coated CFs with M = Ti + Cr after fire exposure, **(b)** EDS maps of the coated CFs, and **(c)** EDS quantification of EDS map area

In addition, structural information on the virgin CFs and CFs with multilayer coating after fire exposure were characterized using Raman spectroscopy. The Raman spectra of CFs in **Figure S11** show two peaks around 1350 and 1580 cm^{-1} related to disorder/defects in the carbon structures and ordered graphite structure which are named D- and G-bands, respectively (6). Based on the D- and G-band ratio (I_D/I_G), the graphitization of the CFs can be estimated. It was found that the I_D/I_G ratio was about ~0.9 for the original CFs and those after the oxidation test. This result implies that the structures of the CFs remained intact after the fire test and thus, demonstrate the high fire-resistance performance of the multiyear coating as on the carbon materials.

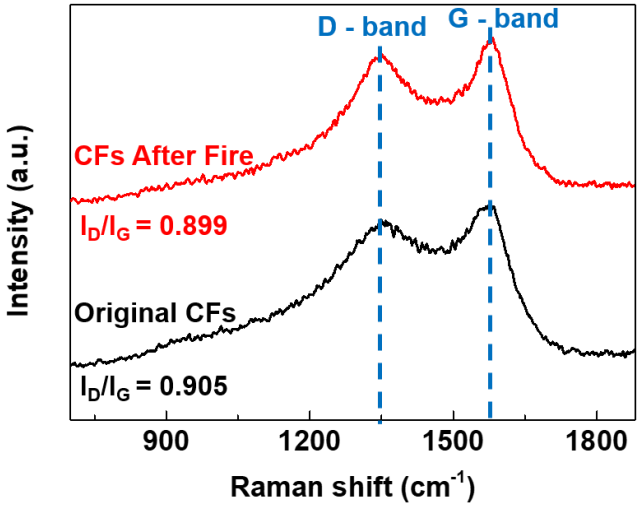

Figure S11. Raman spectra of original CFs and multilayer coated fibers after fire exposure.

References:

1. T. Arai, Carbide coating process by use of molten borax bath in Japan. *J. Heat Treating* **1**, 15–22 (1979).

2. J. Roger, F. Audubert, Y. Le Petitcorps, Thermal reaction of SiC films with tungsten and tungsten–rhenium alloys. *J Mater Sci* **43**, 3938–3945 (2008).

3. S. Kasimuthumaniyan, S. K. Singh, K. Jayasankar, K. Mohanta, A. Mandal, An alternate approach to synthesize TiC powder through thermal plasma processing of titania rich slag. *Ceramics International* **42**, 18004–18011 (2016).

4. J. I. Peña-Flores, *et al.*, Fe effect on the optical properties of TiO2:Fe2O3 nanostructured composites supported on SiO2 microsphere assemblies. *Nanoscale Res Lett* **9**, 499 (2014).

5. M. Mohammadtaheri, Q. Yang, Y. Li, J. Corona-Gomez, The Effect of Deposition Parameters on the Structure and Mechanical Properties of Chromium Oxide Coatings Deposited by Reactive Magnetron Sputtering. *Coatings* **8**, 111 (2018).

6. M. Zhao, *et al.*, Interfacially reinforced carbon fiber/epoxy composites by grafting melamine onto carbon fibers in supercritical methanol. *RSC Adv.* **6**, 29654–29662 (2016).